Preoperative Localization of Adenomas in Primary Hyperparathyroidism: The Value of ^{11}C-Choline PET/CT in Patients with Negative or Discordant Findings on Ultrasonography and ^{99m}Tc-Sestamibi SPECT/CT

Yimin Liu[1,2], Yonghong Dang[1,2], Li Huo*[1,2], Ya Hu[3], Ou Wang[4], He Liu[5], Xiaoyan Chang[6], Yu Liu[1,2], Xiaoping Xing[4], Fang Li[1,2], Quan Liao[3], Marcus Hacker[7], Xiang Li*[7], and Michael C. Kreissl*[8]

[1]Department of Nuclear Medicine, Peking Union Medical College Hospital, Chinese Academy of Medical Science and Peking Union Medical College, Peking, China; [2]Department of Nuclear Medicine, Beijing Key Laboratory of Molecular Targeted Diagnosis and Therapy in Nuclear Medicine, Beijing, China; [3]Department of Surgery, Peking Union Medical College Hospital, Chinese Academy of Medical Science and Peking Union Medical College, Peking, China; [4]Department of Endocrinology, Peking Union Medical College Hospital, Chinese Academy of Medical Science and Peking Union Medical College, Peking, China; [5]Department of Ultrasound, Peking Union Medical College Hospital, Chinese Academy of Medical Science and Peking Union Medical College, Peking, China; [6]Department of Pathology, Peking Union Medical College Hospital, Chinese Academy of Medical Science and Peking Union Medical College, Peking, China; [7]Division of Nuclear Medicine, Department of Biomedical Imaging and Image-Guided Therapy, Medical University of Vienna, Vienna, Austria; and [8]Department of Radiology and Nuclear Medicine, University Hospital Magdeburg, Magdeburg, Germany

We aimed to assess the value of ^{11}C-choline PET in patients with primary hyperparathyroidism and negative or discordant results on ^{99m}Tc-sestamibi imaging and neck ultrasound. **Methods:** Eighty-seven such patients were assessed and subsequently underwent parathyroidectomy. PET/CT image data were analyzed semiquantitatively using SUV_{max} and SUV ratios (target to contralateral thyroid gland and carotid artery). A positive PET/CT result was defined as focal uptake significantly higher than regular thyroid tissue. Ectopic foci were also considered positive. Inconclusive PET/CT cases were defined as a lesion with uptake equal to normal thyroid tissue. If no prominent or ectopic uptake was detectable, the PET/CT result was considered negative. **Results:** When dichotomizing the ^{11}C-choline PET/CT imaging results by defining lesions with both positive and inconclusive uptake as positive, we found 84 of 92 lesions (91.3%) to have true-positive uptake whereas 8 lesions (8.7%) had false-positive uptake. One lesion showed false-negative uptake; the sensitivity was 98.8%. The corresponding positive predictive value for lesions was 91.3%. The mean SUV_{max} was 6.15 ± 4.92 in 72 lesions with positive uptake (70 patients) and 2.96 ± 2.32 in 20 lesions with inconclusive uptake (18 patients). **Conclusion:** These results in a large group of patients indicate that ^{11}C-choline PET/CT is a promising tool for parathyroid adenoma localization when ultrasound and ^{99m}Tc-sestamibi imaging yield negative or discordant results.

Key Words: ^{11}C-choline; PET/CT; primary hyperparathyroidism

J Nucl Med 2020; 61:584–589
DOI: 10.2967/jnumed.119.233213

For correspondence or reprints contact: Li Huo, Department of Nuclear Medicine, Peking Union Medical College (PUMC) Hospital, Chinese Academy of Medical Science & PUMC, Beijing, China.
E-mail: huoli@pumch.cn
*Contributed equally to this work.
Published online Oct. 10, 2019.
COPYRIGHT © 2020 by the Society of Nuclear Medicine and Molecular Imaging.

In primary hyperparathyroidism, preoperative localization of hyperfunctioning parathyroid adenomas (PTAs) is necessary for planning surgery. Neck ultrasound and ^{99m}Tc-sestamibi parathyroid scintigraphy with and without SPECT/CT are currently the most commonly used imaging tools (*1,2*). Neck ultrasound has the advantages of being noninvasive, low-cost, and widely available. It is also not associated with any radiation exposure and can be used to assess coexisting thyroid nodules (*2*). The sensitivity of ultrasound for the detection of PTAs is, however, highly variable and has been reported to be between 57% and 76% (*3–5*). Ectopic PTAs or PTAs deep in the tissue pose a problem for this imaging method (*6,7*).

Parathyroid imaging using ^{99m}Tc-sestamibi, preferably including hybrid imaging with SPECT/CT, is also noninvasive and available in most centers, but it is associated with radiation exposure. The sensitivities reported, mainly in retrospective studies using SPECT/CT, are mostly superior to those of neck ultrasound alone and range from 53% to 92% (*4,7–9*). ^{99m}Tc-sestamibi imaging has the advantage over ultrasound of being able to also detect ectopic PTAs or PTAs located deeper within the neck. However, thyroid nodules may also show increased ^{99m}Tc-sestamibi uptake, and an association between thyroid disease—that is, nodular goiter or toxic nodular goiter—and parathyroid disease is quite common (*10*). This can create difficulty in identifying PTAs. Many institutions combine neck ultrasound and parathyroid scintigraphy, which increases sensitivity to 80%–90% (*11–13*). If the adenoma can be found preoperatively by imaging, minimally invasive surgery may be performed in many cases. If the adenoma cannot be clearly localized before surgery, the surgeon usually has to find and inspect all parathyroid glands, which requires a significantly more extensive surgery and, thus, makes the patient more prone to morbidity. Also, ectopic PTAs cannot be detected this way. Therefore, problems arise if neither imaging modality can locate the PTA or if the results obtained by imaging are inconclusive or discordant. ^{11}C-methionine PET/CT has

been successfully applied in this setting (*14–18*). During the last few years, radiolabeled choline has been increasingly used to localize PTAs, with high sensitivities reported (*19–22*). However, many studies were conducted on small patient cohorts. Our aim was to evaluate the utility of ^{11}C-choline in a large cohort of patients with negative, inconclusive, or discordant results on neck ultrasound and ^{99m}Tc-sestamibi scintigraphy, including SPECT/CT. The imaging results were correlated with histopathologic results.

MATERIALS AND METHODS

Patients

Eighty-seven patients with biologically proven primary hyperparathyroidism (elevated parathyroid hormone [PTH] levels or normal PTH despite hypercalcemia) and negative or discordant results on neck ultrasound and ^{99m}Tc-sestamibi SPECT/CT were assessed using ^{11}C-choline PET/CT and underwent parathyroidectomy. All patients gave written informed consent for the procedure. The exclusion criteria were profound vitamin D deficiency and severe kidney failure (creatinine clearance $<$ 30 mL/min). The data were analyzed retrospectively. The local ethics committee approved the data analysis.

Neck Ultrasound

The patients were imaged supine with neck extended using a high-frequency linear transducer. The assessment included the area from the mandible to the sternal notch bilaterally. Longitudinal and transverse views were used to locate the parathyroid glands suspected of being abnormal (homogeneous hypoechoic lesions that are oval or bean-shaped). Also, the presence or absence of thyroid nodules was documented in all patients. Ultrasonography was performed and reported by 2 experienced radiologists. The results in terms of PTA detection were categorized into positive, negative, or inconclusive cases.

^{99m}Tc-Sestamibi Imaging and Analysis

The patients were injected intravenously with 740 MBq ± 20 MBq of ^{99m}Tc-sestamibi (Atom Hitech Co., Ltd.). Early and late planar images were acquired at, respectively, 20 min and 2 h after radiotracer administration, using a conventional γ-camera with a pinhole collimator [200,000 counts during early and late acquisitions] (E.CAM; Siemens Medical Solutions). In addition, SPECT/CT data were acquired on a 64-slice Philips Precedence device after the second acquisition of planar images (CT: 30 mAs, 120 kV, 3-mm slice thickness; SPECT: low-energy high-resolution collimator, 128 × 128 matrix, zoom of 1.0).

The planar images and SPECT/CT data were reviewed for parathyroid visualization by an experienced nuclear medicine physician, and a negative ^{99m}Tc-sestamibi result was defined as the absence of focal uptake on the early or delayed images. An inconclusive ^{99m}Tc-sestamibi SPECT/CT result was defined as only vague uptake in the soft tissue adjacent to the thyroid, or uptake possibly associated with thyroid nodules.

Evaluation of Imaging Procedures Before PET Imaging

Subsequently, the results of ultrasound and ^{99m}Tc-sestamibi imaging were reviewed.

PET/CT was performed if both ultrasound and ^{99m}Tc-sestamibi imaging were negative or if the results of the 2 modalities were deemed discordant. This was the case if a positive or inconclusive result by one imaging modality could not be confirmed by the other modality (was negative or inconclusive). Also, if there was a discrepancy in the number or location of lesions between the 2 modalities, the results were rated as discordant.

^{11}C-Choline PET/CT and Analysis

Twenty minutes after intravenous injection of ^{11}C-choline (385 ± 175 MBq), a low-dose CT scan was performed (30–70 mAs, 120 kV, 5-mm slices, pitch of 0.8), followed by a 2- to 3-bed-position PET acquisition of 6–9 min covering the neck and upper chest using a 3-dimensional Biograph 64 PET/CT system (Siemens). The injected activity and the exact time between injection and the start of image acquisition were recorded. The effective dose attributable to the low-dose CT was calculated by multiplying the conversion factor of 0.0059 mSv/mGy/cm by the dose–length product; the effective dose due to the ^{11}C-choline administration was calculated by multiplication of the injected dose in megabecquerels by the conversion factor 0.00435 mSv/MBq (*23*).

The raw PET data were reconstructed with 2 iterations, 8 subsets, point-spread-function (PSF) reconstruction, a 168 × 168 matrix, and a zoom of 1.0. Scatter and attenuation corrections were applied. PET/CT imaging data were reviewed by *2* experienced nuclear physicians masked to other imaging data and reports. A semiquantitative assessment based on a visual interpretation was performed. A positive ^{11}C-choline PET/CT scan was defined as a clear focus of uptake, which, on

TABLE 1
Patient Characteristics

Characteristic	Data	Reference range
Sex		
Male	27 (31%)	
Female	60 (69%)	
Age (y)	56.0 ± 12.6	
Body mass index	24.6 ± 3.7	
Previous thyroidectomy	5 (5.7%)	
Previous parathyroidectomy	5 (5.7%)	
Biochemistry		
Calcium (mmol/L)	2.73 ± 0.23	2.13–2.70
PTH (pg/mL)	254.5 ± 303.1	12.0–65.0
Albumin (g/L)	43 ± 4	35–51
Phosphorus (mmol/L)	0.85 ± 0.18	0.81–1.45
25-hydroxyvitamin D (ng/mL)	14.2 ± 7.0	8.0–50.0
Creatinine (μmol/L)	72 ± 27	59–104
Alkaline phosphatase (U/L)	151 ± 206	30–120

Qualitative data are expressed as numbers; continuous data are expressed as mean ± SD.

TABLE 2
Results of Ultrasonography and ^{99m}Tc-Sestamibi Imaging

Modality	*n*
Ultrasonography	
Negative	15 (17%)
Inconclusive	36 (41.4%)
Thyroid nodules	54 (62.1%)
^{99m}Tc-sestamibi imaging, including SPECT/CT	
Negative	40 (46.0%)
Inconclusive	27 (31.0%)

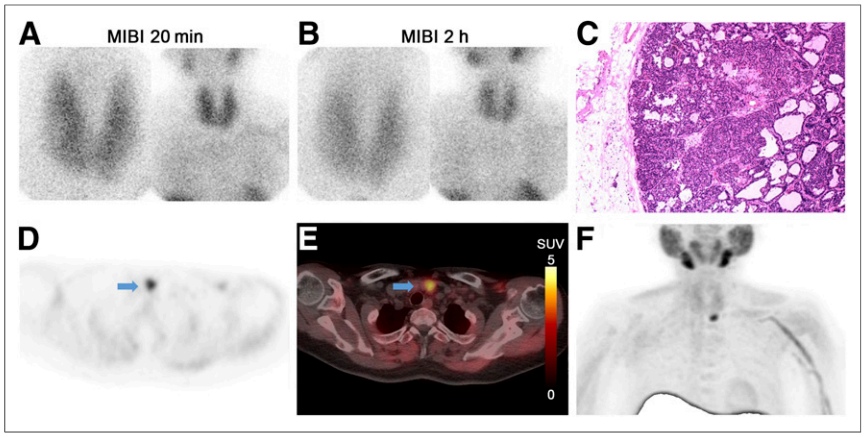

FIGURE 1. Representative positive PET scan of 43-y-old man with PTH level of 1,358 pg/mL, serum calcium level of 3.0 mmol/L, phosphate level of 0.78 mmol/L, alkaline phosphatase level of 82 U/L, and creatinine level of 98 μmol/L. Neck ultrasound imaging showed suspected 1.8 × 1.5 × 0.7 cm nodule at left thyroid lobe region. (A and B) Negative findings on ^{99m}Tc-sestamibi imaging of neck at 20 min and 2 h after injection. (C) Histopathologic assessment: encapsulated PTA, which is composed predominantly of chief cells with pseudoglandular architecture in keeping with PTA. (D and E) Transverse views of ^{11}C-choline PET/CT; arrows indicate PTA with strong uptake of ^{11}C-choline (size on CT, 1.1 × 1.3 × 1.4 cm; SUV_{max}, 6.87; SUV_{mean} of contralateral thyroid, 2.03; SUV_{mean} of contralateral carotid artery, 0.67). (F) Maximum-intensity projection of ^{11}C-choline PET. MIBI = ^{99m}Tc-sestamibi.

visual interpretation, was significantly higher than uptake by regular thyroid tissue. Ectopic focal uptake, distant from the thyroid or thyroid bed, was also considered a positive PET result. Inconclusive PET/CT cases were defined as a soft-tissue lesion with uptake in the same range as that of normal thyroid tissue. If no prominent or ectopic uptake was detectable, the PET/CT scan was considered to be negative.

The SUV_{max} of the PTAs was measured by assigning a spheric volume of interest with a diameter of 10 mm to the area of suspected uptake using the PET Edge tool (Siemens). The SUV_{mean} of the background was measured by placing a spheric volume of interest with same diameter inside the contralateral thyroid lobe as well as on the contralateral carotid artery. The SUV ratios (SUVRs) were calculated using the 2 background regions. Receiver-operating-characteristic analysis was used to determine the optimal cutoff for SUVR in predicting true PTA lesions. Sensitivity, specificity, and accuracy for predicting true PTA lesions were also calculated.

Surgery and PTH-Level Examination

Surgery was performed between 1 and 20 wk after ^{11}C-choline PET/CT. The surgeons were aware of the outcome of the imaging results. If the PTA could not be localized intraoperatively by minimally invasive surgery, the surgeons proceeded to bilateral neck exploration. The intraoperative location of the PTA was recorded and correlated with the results of PET/CT. Patients received additional thyroidectomy when a goiter or a large dominant thyroid nodule was present. All patients were discharged from the hospital within 1–2 d. PTH levels and serum calcium levels were determined during hospitalization. Successful parathyroidectomy was defined as a greater than 50% decrease in intraoperative PTH level 10 min after parathyroidectomy, or normalization of PTH level postoperatively at first follow-up along with the presence of abnormal parathyroid tissue at pathologic examination.

Histology

Histologic analysis was performed on sections taken from paraffin-embedded tissue stained with hematoxylin and eosin. Immunohistochemistry with anti-PTH antibody was performed. PTA and parathyroid hyperplasia were considered a true-positive result.

Statistical Analysis

Quantitative variables are described as mean ± SD, whereas qualitative variables are described as numbers and percentages. For group comparisons, unpaired Student *t* tests were used for parametric variables, and the Mann–Whitney *U* test was used for nonparametric variables.

Sensitivity, specificity, and accuracy were calculated by χ^2 testing. All statistical analyses were performed using SPSS, version 23 (IBM). *P* values of less than 0.05 were considered statistically significant.

RESULTS

Patient Characteristics

In total, 87 patients with primary hyperparathyroidism could be included in the analysis. Patient characteristics, including laboratory values (Table 1) and results of ultrasound and ^{99m}Tc-sestamibi imaging (Table 2), are provided.

^{11}C-Choline Imaging

The mean delay between injection and image acquisition was 25 ± 5 min. Effective doses due to the ^{11}C-choline injection

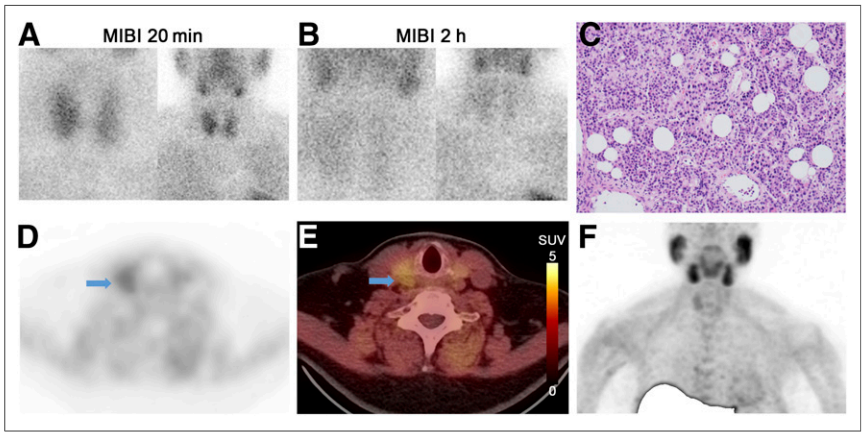

FIGURE 2. Representative inconclusive PET scan from 52-y-old woman with PTH level of 138 pg/mL, serum calcium level of 2.95 mmol/L, phosphate level of 0.9 mmol/L, alkaline phosphatase level of 130 U/L, and creatinine level of 61 μmol/L. Neck ultrasound showed suspected lesion next to right thyroid lobe, measuring 2.2 × 1.5 × 0.6 cm. (A and B) Negative findings on ^{99m}Tc-sestamibi scan at 20 min and 2 h after injection. (C) Histopathologic assessment: parathyroid tissue with hypercellularity, which is composed mainly of chief cells and adipocytes, consistent with PTA. (D and E) Transverse views of ^{11}C-choline PET/CT; arrows indicate inconclusive focus of ^{11}C-choline uptake suspected of being PTA (size on CT, 0.9 × 0.8 × 0.8 cm; SUV_{max}, 2.16; SUV_{mean} of contralateral thyroid, 2.01; SUV_{mean} of contralateral carotid artery, 0.97). (F) Maximum-intensity projection of ^{11}C-choline PET. MIBI = ^{99m}Tc-sestamibi.

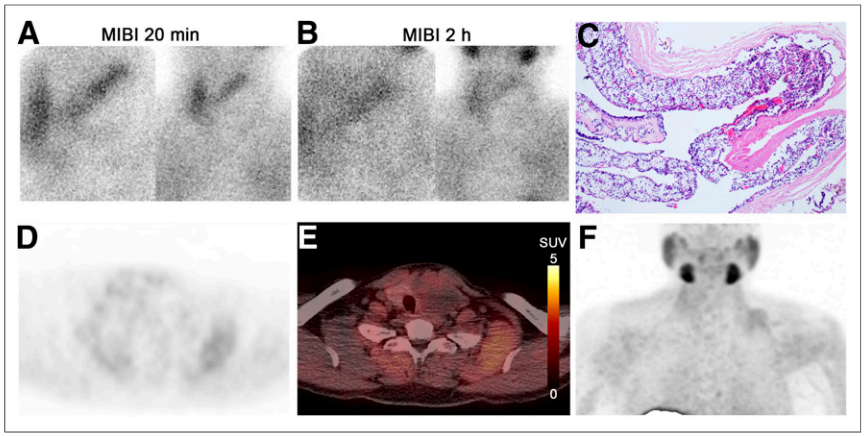

FIGURE 3. Representative negative PET from 39-y-old man with PTH level of 140.1 pg/mL, serum calcium level of 2.74 mmol/L, phosphate level of 0.68 mmol/L, alkaline phosphatase level of 75 U/L, and creatinine level of 111 μmol/L. Neck ultrasound showed apparently nodular, cystic, and enlarged left thyroid lobe with dimensions of 7.7 × 5.5 × 3.7 cm. (A and B) Negative findings on ^{99m}Tc-sestamibi scan at 20 min and 2 h after injection. (C) Histopathologic assessment: encapsulated hypercellular parathyroid tissue, which is composed of water clear cells. Final diagnosis was PTA with extensive cystic degeneration. (E and F) Transverse views of ^{11}C-choline PET/CT, negative for uptake (SUV_{mean} of contralateral thyroid, 1.44; SUV_{mean} of contralateral carotid artery, 1.86). On CT, cystic lesion was visualized in left thyroid region. (F) Maximum-intensity projection of ^{11}C-choline PET. MIBI = ^{99m}Tc-sestamibi.

and the low-dose CT were calculated to be 1.7 ± 0.8 mSv and 2.5 ± 1.5 mSv, respectively. In 86 patients, ^{11}C-choline PET/CT visualized 92 positive foci, including 20 foci with inconclusive uptake; on CT, the lesions had a mean maximum transverse diameter of 13.7 ± 7.0 mm. Representative examples of a positive scan (Fig. 1), an inconclusive scan (Fig. 2), and a negative scan (Fig. 3) are shown.

Of 92 lesions with positive and inconclusive uptake, the lesional SUV_{max}, the background SUV_{mean} for the carotid and thyroid, and the lesion-to-background SUVRs are listed in Table 3. For 72 PET lesions with positive uptake in 70 patients, the mean SUV_{max} was 6.15 ± 4.92 and the mean SUVR for the carotid and thyroid were 4.49 ± 2.68 and 2.22 ± 1.18, respectively. For 20 lesions with inconclusive uptake in 18 patients, a mean SUV_{max} of 2.96 ± 2.32, a mean SUVR of 2.68 ± 0.98 for the carotid, and a mean SUVR of 1.37 ± 0.33 for the thyroid were calculated. One patient had 1 lesion with positive uptake and 1 lesion with inconclusive uptake (Table 3). SUVR cutoffs of 2.84 for the carotid and 1.67 for the thyroid were determined by receiver-operating-characteristic analysis.

Diagnostic Performance

When dichotomizing the ^{11}C-choline PET/CT imaging results by defining lesions with both positive and inconclusive uptake as positive ^{11}C-choline PET lesions, we found that 84 of 92 lesions (91.3%) had true-positive uptake, versus 8 lesions (8.7%) that had false-positive uptake. One lesion had false-negative uptake, with sensitivity of 98.8 (95% confidence interval, 92.7–99.9) (Table 4). The corresponding per-lesion positive predictive value was 91.3% (95% confidence interval, 83.1–95.9). An SUVR cutoff of 2.84 for the carotid yielded a sensitivity of 58.3%, specificity of 75.0%, and accuracy of 61.3%. In comparison, the SUVR cutoff of 1.37 for the thyroid yielded a sensitivity of 56.0%, specificity of 87.5%, and accuracy of 65.2%. Detailed histologic results can be found in Table 4.

PTH Level After Surgery

The PTH levels in most patients with positive choline uptake (67/70 patients) and patients with inconclusive uptake (15/16) showed a significant decrease (>50%) after surgery. The detailed results are listed in Table 5.

DISCUSSION

To the best of our knowledge, this was the largest cohort of patients examined with ^{11}C-choline thus far. All patients had, according to the laboratory parameters obtained, primary hyperparathyroidism and negative or inconclusive results on ultrasound and ^{99m}Tc-sestamibi imaging (including SPECT/CT); the correlation with histology was determined for all patients. Our retrospective analysis showed that ^{11}C-choline PET/CT can help identify the location of PTAs in the studied group of patients because of its high sensitivity and positive predictive value for the location of PTAs.

In previous studies, ^{11}C-methionine has been shown to be of great value, especially, but not only, in the setting of negative

TABLE 3
Values in Lesions with Positive and Inconclusive ^{11}C-Choline Uptake

Parameter	Positive uptake (n = 72)	Inconclusive uptake (n = 20)	Total (n = 92)
SUV_{max} of lesions	6.15 ± 4.92*	2.96 ± 2.32	5.45 ± 4.67
Background SUV_{mean}			
Contralateral thyroid	2.84 ± 1.91	2.14 ± 1.44	2.69 ± 1.83
Contralateral carotid artery	1.39 ± 0.79	1.03 ± 0.39	1.31 ± 0.74
Lesion target-to-background SUVR			
Thyroid	2.22 ± 1.18*	1.37 ± 0.33	2.03 ± 1.11
Carotid	4.49 ± 2.68*	2.68 ± 0.98	4.09 ± 2.52

*$P < 0.001$ (positive lesions vs. inconclusive lesions).
Data are mean ± SD.

TABLE 4
Histopathologic Results for All Lesions (n = 93)

^{11}C-choline finding	Parathyroid glands (n = 85)	Nonparathyroid lesions (n = 8)
Lesions positive for uptake (n = 72)	Lesions with true-positive PET uptake (n = 67, 93.06%)	Lesions with false-positive PET uptake (n = 5, 6.94%)
	Histology: 53 PTA; 14 parathyroid hyperplasia	Histology: 3 nodular goiter; 1 thymoma; 1 normal parathyroid tissue
Lesions inconclusive for uptake (n = 20)	Lesions with true-positive PET uptake (n = 17, 85%)	Lesions with false-positive PET uptake (n = 3, 15%)
	Histology: 10 PTA; 7 parathyroid hyperplasia	Histology: 2 nodular goiter; 1 follicular nodule
Lesions negative for uptake (n = 1)	Lesions with false-negative PET uptake (n = 1, 100%)	
	Histology: 1 cystic PTA	

^{99m}Tc-sestamibi results (*14–17*). The pooled sensitivity in a meta-analysis of 9 studies with a total of 137 patients was found to be 86% (*24*). When the thyroid SUVR is compared with the data published by Otto et al. (*25*), the value they reported, 1.8 at 40 min after injection, is slightly lower than the value we observed. The background ratio in that study, up to 2.8, is smaller than the carotid SUVR in our study; however, the group used soft tissue as a reference. All in all, according to our data, ^{11}C-choline imaging seems to perform at least as well as ^{11}C-methionine in the detection of PTAs. However, a head-to-head-comparison is needed to assess whether the method is indeed superior.

The data we obtained are in keeping with the published data using ^{18}F-fluorocholine PET/CT and with the only larger study published thus far using ^{11}C-choline PET/CT.

In 2014, Orevi et al. published a study using ^{11}C-choline PET/CT in 40 patients (*21*). The results correlated with other imaging modalities—in particular, with ^{99m}Tc-sestamibi imaging also. In 93% of cases, a PTA could be visualized. The results of PET and ^{99m}Tc-sestamibi imaging were concordant in 29 cases; PET clearly outperformed ^{99m}Tc-sestamibi imaging. In our study, we could not test for a correlation with ^{99m}Tc-sestamibi, since only cases with negative or inconclusive ^{99m}Tc-sestamibi imaging and ultrasound results were included. Nevertheless, the detection rate for ^{11}C-choline PET/CT in our study was even higher (99%). However, a selection bias cannot be excluded.

Michaud et al. used ^{18}F-fluorocholine PET/CT in a small patient collective that was more comparable to ours, with equivocal or discordant results on ultrasound and ^{99m}Tc-sestamibi imaging; however, patients who also had secondary hyperparathyroidism were included (*26*). On a per-patient basis, a sensitivity of 88% for open reading and 94% for masked reading was observed; these values are slightly lower than the ones in our study. Also, in terms of quantitation, a mean SUV_{max} of 3.9 and a thyroid SUVR of 1.5 were determined in that trial. Using ^{11}C-choline, we found significantly higher values, with a mean SUV_{max} of 6.1 and a thyroid SUVR of 2.2 in the positive cases.

Using a similar small patient collective, but implementing ^{18}F-fluorocholine PET/MR, Kluijfhout et al. reported a per-lesion sensitivity of 90%, remarkably without any false-positive findings (*27*). In our study, 8 of 92 lesions were false-positive. In the PET/MR study of Kluijfhout et al., the mean SUV_{max} was found to be a bit higher (4.2) than in the study using PET/CT (*26*).

As in most studies, our study visually analyzed image data in order to detect PTAs. When receiver-operating-characteristic analysis was used to determine the optimal cutoff for carotid and thyroid SUVR, the results for sensitivity, specificity, and accuracy for predicting true PTA lesions were clearly inferior to visual analysis.

Of course, several limitations of our study have to be pointed out. The most prominent limitation is the retrospective study design, which could potentially lead to a selection bias. In addition, a selection bias can be expected because only patients who underwent surgery were analyzed. Also, only 1 type of PET/CT scan, with a specified reconstruction algorithm, was used. On one hand, this criterion results in homogeneous data, but on the other hand, the results for the SUVs and ratios cannot be readily applied to other institutions with different types of PET/CT scans or other reconstruction algorithms. Because the data were interpreted mainly visually, much as in ^{99m}Tc-sestamibi imaging, this limitation can be rated as a minor one.

Another limitation is that, because of the short half-life of ^{11}C, late imaging was not feasible in our study. A combination of early and delayed imaging was recently shown to detect additional PTAs using ^{18}F-fluorocholine PET/CT in a large collective of 64 patients (*28*). A direct comparison cannot be made because of differences in the patient collective and study setup; however,

TABLE 5
PTH Level After Surgery

^{11}C-choline finding	PTH level after surgery
Lesions positive for choline uptake (n = 70)	Group 1 (n = 1) (no difference)
	Group 2 (n = 2) (decreasing 30%–50%)
	Group 3 (n = 67) (decreasing > 50%)
Lesions inconclusive for choline uptake (n = 16)	Group 1 (n = 1) (decreasing 42%)
	Group 1 (n = 15) (decreasing > 50%)
Lesions negative for choline uptake (n = 1)	Group 4 (n = 1) (decreasing > 50%)

even when the inconclusive cases are included, the ratio of parathyroid to normal thyroid tissue in our study appears to be at least as high as the ratio in the above-mentioned study (*28*).

CONCLUSION

These results in a large group of patients indicate that ^{11}C-choline PET/CT is a promising tool for PTA localization when ultrasound and ^{99m}Tc-sestamibi imaging, including SPECT/CT, yield negative or discordant results. However, the reported data on the diagnostic accuracy of ^{11}C-choline PET/CT for parathyroid imaging cannot reflect the true diagnostic accuracy in clinical practice because of the obvious referral bias of the study. Furthermore, it is not possible to compare the imaging accuracy with that of ^{99m}Tc-sestamibi SPECT imaging, since no head-to-head comparison was performed.

DISCLOSURE

This work was sponsored in part by the National Natural Science Foundation of China (grant 81571713), the CAMS Innovation Fund for Medical Sciences (CIFMS) (grant 2016-I2M-4-003), and the CAMS Initiative for Innovative Medicine (CAMS-2018-I2M-3-001). No other potential conflict of interest relevant to this article was reported.

KEY POINTS

QUESTION: What is the utility of ^{11}C-choline PET in the detection of PTAs in primary hyperparathyroidism?

PERTINENT FINDINGS: In this retrospective analysis of a large cohort of patients with primary hyperparathyroidism and negative or inconclusive results on ultrasound and ^{99m}Tc-sestamibi imaging, ^{11}C-choline PET/CT showed a positive predictive value of 91.3% for lesions, with a high sensitivity of 98.8%.

IMPLICATIONS FOR PATIENT CARE: ^{11}C-choline PET/CT is suitable for detecting hyperfunctioning parathyroid tissue in patients with primary hyperparathyroidism.

REFERENCES

1. Frank E, Ale-Salvo D, Park J, Liu Y, Simental A Jr, Inman JC. Preoperative imaging for parathyroid localization in patients with concurrent thyroid disease: a systematic review. *Head Neck.* 2018;40:1577–1587.
2. Alexandrides TK, Kouloubi K, Vagenakis AG, et al. The value of scintigraphy and ultrasonography in the preoperative localization of parathyroid glands in patients with primary hyperparathyroidism and concomitant thyroid disease. *Hormones (Athens).* 2006;5:42–51.
3. Bhansali A, Masoodi SR, Bhadada S, Mittal BR, Behra A, Singh P. Ultrasonography in detection of single and multiple abnormal parathyroid glands in primary hyperparathyroidism: comparison with radionuclide scintigraphy and surgery. *Clin Endocrinol (Oxf).* 2006;65:340–345.
4. Cheung K, Wang TS, Farrokhyar F, Roman SA, Sosa JA. A meta-analysis of preoperative localization techniques for patients with primary hyperparathyroidism. *Ann Surg Oncol.* 2012;19:577–583.
5. Lo CY, Lang BH, Chan WF, Kung AW, Lam KS. A prospective evaluation of preoperative localization by technetium-99m sestamibi scintigraphy and ultrasonography in primary hyperparathyroidism. *Am J Surg.* 2007;193:155–159.
6. Harari A, Mitmaker E, Grogan RH, et al. Primary hyperparathyroidism patients with positive preoperative sestamibi scan and negative ultrasound are more likely to have posteriorly located upper gland adenomas (PLUGs). *Ann Surg Oncol.* 2011;18:1717–1722.
7. Ciappuccini R, Morera J, Pascal P, et al. Dual-phase ^{99m}Tc sestamibi scintigraphy with neck and thorax SPECT/CT in primary hyperparathyroidism: a single-institution experience. *Clin Nucl Med.* 2012;37:223–228.
8. Lavely WC, Goetze S, Friedman KP, et al. Comparison of SPECT/CT, SPECT, and planar imaging with single- and dual-phase ^{99m}Tc-sestamibi parathyroid scintigraphy. *J Nucl Med.* 2007;48:1084–1089.
9. Neumann DR, Obuchowski NA, Difilippo FP. Preoperative ^{123}I/^{99m}Tc-sestamibi subtraction SPECT and SPECT/CT in primary hyperparathyroidism. *J Nucl Med.* 2008;49:2012–2017.
10. Campenni A, Giovinazzo S, Pignata SA, et al. Association of parathyroid carcinoma and thyroid disorders: a clinical review. *Endocrine.* 2017;56:19–26.
11. Patel CN, Salahudeen HM, Lansdown M, Scarsbrook AF. Clinical utility of ultrasound and ^{99m}Tc sestamibi SPECT/CT for preoperative localization of parathyroid adenoma in patients with primary hyperparathyroidism. *Clin Radiol.* 2010;65:278–287.
12. Steward DL, Danielson GP, Afman CE, Welge JA. Parathyroid adenoma localization: surgeon-performed ultrasound versus sestamibi. *Laryngoscope.* 2006;116:1380–1384.
13. Sukan A, Reyhan M, Aydin M, et al. Preoperative evaluation of hyperparathyroidism: the role of dual-phase parathyroid scintigraphy and ultrasound imaging. *Ann Nucl Med.* 2008;22:123–131.
14. Noltes ME, Coester AM, van der Horst-Schrivers ANA, et al. Localization of parathyroid adenomas using ^{11}C-methionine PET after prior inconclusive imaging. *Langenbecks Arch Surg.* 2017;402:1109–1117.
15. Traub-Weidinger T, Mayerhoefer ME, Koperek O, et al. ^{11}C-methionine PET/CT imaging of ^{99m}Tc-MIBI-SPECT/CT-negative patients with primary hyperparathyroidism and previous neck surgery. *J Clin Endocrinol Metab.* 2014;99:4199–4205.
16. Braeuning U, Pfannenberg C, Gallwitz B, et al. ^{11}C-methionine PET/CT after inconclusive ^{99m}Tc-MIBI-SPECT/CT for localisation of parathyroid adenomas in primary hyperparathyroidism. *Nuklearmedizin.* 2015;54:26–30.
17. Weber T, Maier-Funk C, Ohlhauser D, et al. Accurate preoperative localization of parathyroid adenomas with C-11 methionine PET/CT. *Ann Surg.* 2013;257:1124–1128.
18. Weber T, Cammerer G, Schick C, et al. C-11 methionine positron emission tomography/computed tomography localizes parathyroid adenomas in primary hyperparathyroidism. *Horm Metab Res.* 2010;42:209–214.
19. Piccardo A, Trimboli P, Rutigliani M, et al. Additional value of integrated ^{18}F-choline PET/4D contrast-enhanced CT in the localization of hyperfunctioning parathyroid glands and correlation with molecular profile. *Eur J Nucl Med Mol Imaging.* 2019;46:766–775.
20. Quak E, Blanchard D, Houdu B, et al. F18-choline PET/CT guided surgery in primary hyperparathyroidism when ultrasound and MIBI SPECT/CT are negative or inconclusive: the APACH1 study. *Eur J Nucl Med Mol Imaging.* 2018;45:658–666.
21. Orevi M, Freedman N, Mishani E, Bocher M, Jacobson O, Krausz Y. Localization of parathyroid adenoma by ^{11}C-choline PET/CT: preliminary results. *Clin Nucl Med.* 2014;39:1033–1038.
22. Treglia G, Piccardo A, Imperiale A, et al. Diagnostic performance of choline PET for detection of hyperfunctioning parathyroid glands in hyperparathyroidism: a systematic review and meta-analysis. *Eur J Nucl Med Mol Imaging.* 2019;46:751–765.
23. Highlights of prescribing information: Choline C 11 injection, for intravenous use. U.S. Food and Drug Administration website. https://www.accessdata.fda.gov/drugsatfda_docs/label/2012/203155s000lbl.pdf. Published 2012. Accessed December 3, 2019.
24. Jochumsen MR, Iversen P, Arveschoug AK. Follicular thyroid cancer avid on C-11 methionine PET/CT. *Endocrinol Diabetes Metab Case Rep.* 2018;2018:17-0151.
25. Otto D, Boerner AR, Hofmann M, et al. Pre-operative localisation of hyperfunctional parathyroid tissue with ^{11}C-methionine PET. *Eur J Nucl Med Mol Imaging.* 2004;31:1405–1412.
26. Michaud L, Balogova S, Burgess A, et al. A pilot comparison of ^{18}F-fluorocholine PET/CT, ultrasonography and ^{123}I/^{99m}Tc-sestaMIBI dual-phase dual-isotope scintigraphy in the preoperative localization of hyperfunctioning parathyroid glands in primary or secondary hyperparathyroidism: influence of thyroid anomalies. *Medicine (Baltimore).* 2015;94:e1701.
27. Kluijfhout WP, Pasternak JD, Gosnell JE, et al. ^{18}F fluorocholine PET/MR imaging in patients with primary hyperparathyroidism and inconclusive conventional imaging: a prospective pilot study. *Radiology.* 2017;284:460–467.
28. Broos WAM, Wondergem M, van der Zant FM, Knol RJJ. Dual-time-point ^{18}F-fluorocholine PET/CT in parathyroid imaging. *J Nucl Med.* 2019;60:1605–1610.